Approximate Maximum Likelihood Time-Delay Estimation for Two Closely Spaced Sources

Article *in* Signal Processing · April 2023

DOI: 10.1016/j.sigpro.2023.109056

Approximate Maximum Likelihood Time-Delay Estimation for Two Closely Spaced Sources

Corentin Lubeigt[a,b,*], François Vincent[b], Lorenzo Ortega[a,c], Jordi Vilà-Valls[b], Eric Chaumette[b]

[a] *TéSA, 7, Boulevard de la Gare, 31500, Toulouse, France*
[b] *ISAE-SUPAERO, 10, Avenue Edouard Belin, 31055, Toulouse, France*
[c] *IPSA, 40, Boulevard de la Marquette, 31000, Toulouse, France*

Abstract

The study of ground reflections of Global Navigation Satellite System (GNSS) signals, as in GNSS Reflectometry (GNSS-R) can lead to the receiver height estimation. The latter is estimated by comparing the time of arrival difference between the direct and reflected signals, also called path separation. In ground-based scenarios, this path separation can be very small, inducing important interference between paths, which makes it difficult to correctly obtain altimetry products. The path separation estimation can be obtained by a brute force dual source maximum likelihood estimator (2S-MLE), but this solution has a large computational cost. On the other hand, the path separation is so small that a number of approximations can be done. In this study, a third order Taylor approximation of the dual source likelihood criterion is proposed to reduce its complexity. The proposed algorithm performance is compared to the non approximated 2S-MLE for the estimation of the path separation, and to a standard single source processing for the estimation of the direct signal time-delay. These results, along with the corresponding lower bounds, prove that the proposed approach may be of interest for two applications: ground-based GNSS-R altimetry (or radar with low elevation targets) and GNSS multipath mitigation.

Keywords: maximum likelihood estimator, joint delay-Doppler estimation, GNSS-R, multipath.

1. Introduction

For almost thirty years, Global Navigation Satellite System (GNSS) signals have been considered not only as a mean to obtain position, velocity and time on Earth, but also as signals of opportunity for scores of applications. For instance, GNSS Reflectometry (GNSS-R) focuses on the reflection of these signals upon the Earth to extract features such as, for the case of ground-based GNSS-R, soil moisture [1], snow depth [2], sea and river heights [3, 4]. The standard model for such applications is to assume a single multipath reflexion on the ground i.e., a specular reflection [5]. Depending on the receiver altitude, the

*Corresponding author
Email address: corentin.lubeigt@tesa.prd.fr (Corentin Lubeigt)

nature of the reflected signal significantly varies. For spaceborne and airborne scenarios, the reflected signal is strongly distorted by the reflecting surface and the atmosphere. On the other hand, for ground-based scenarios, the path separation between the line-of-sight (LOS) and reflected signals is so short that a potential interference between them often happens. Classical GNSS-R techniques that assume direct and reflected paths enough separated do not work in this case. A common approach to study this interference, so-called GNSS Interferometric Reflectometry (GNSS-IR), estimates the fringes of signal-to-noise ratio (SNR) due to the successive constructive and destructive recombinations of the LOS and reflected paths, as the satellite elevation varies [5]. Such a technique uses a single antenna but requires long integration times (some tens of minutes). However, it is less common to try to estimate the parameters of the combined signals in order to extract the path separation from the estimated delays. This is of great interest since it would imply to obtain a GNSS-R product, e.g., the height between receiver and reflecting surface, every tens of milliseconds instead of every few minutes, as it is the case for GNSS-IR. Then the goal of this paper is to provide an alternative to the standard GNSS-IR technique to increase the measurement rate. The challenge is then to estimate the delays of two very closely spaced sources without requiring to interfering techniques. This problem has already been studied for the estimation of the direction of arrival of two closely spaced sources [6, 7]. Based on approximations of the corresponding dual source maximum likelihood estimator (2S-MLE), the complexity of the search is reduced, and in some areas the performance is better than the 2S-MLE's. Other high-resolution time-delay estimation approaches, based on time-delay sparsity [8] and deconvolution [9] of the matched filtered data were also proposed in complex multipath scenarios. Array processing techniques [10, 11] could improve sources separation, but require a hardware complexity increase. Since low-cost applications are targeted, such techniques are not considered in this paper. Finally, the approach proposed in the following focuses on the GNSS-R scenario where only one multipath reflection is considered, it would be interesting to extend it to a larger number of reflections to adapt it to urban navigation applications but this out of the scope of this contribution.

In this communication, an approximation of the 2S-MLE is considered based on a 3^{rd} order Taylor expansion. Such an approximation allows a dimension reduction of the likelihood criterion for the estimation of the time-delays of two closely spaced sources. Based on the shape of the 3^{rd} order approximation, an approximate maximum likelihood estimator (AMLE) is proposed, tested through simulations, and compared to both the 2S-MLE, the corresponding Cramér-Rao bound (CRB) and to a standard single source processing.

2. Signal Model

In this study, a receiver with a single antenna able to collect both a direct signal (indexed 0) and its reflection (indexed 1) is considered. The receiver is assumed close to the ground and the reflection, caused by a smooth surface such as a lake is assumed specular [4]. Refer to Fig. B.1 for an illustration of the

geometry.

2.1. Narrowband Signal Model

Under the ground-based assumptions just mentioned and considering a narrowband band-limited signal sampled at a sampling rate $T_s = 1/F_s$ where F_s, the sampling frequency, is set equal to the RF front-end bandwidth, the received discrete baseband signal is classically identified to a dual source conditional signal model (CSM) [12]:

$$\mathbf{x} = \mathbf{A}(\boldsymbol{\eta}_0, \boldsymbol{\eta}_1)\boldsymbol{\alpha} + \mathbf{w},\ \mathbf{w} \sim \mathcal{CN}(0, \sigma_n^2 \mathbf{I}_N)\ , \tag{1}$$

with, for $i \in \{0, 1\}$, $\boldsymbol{\eta}_i^T = (\tau_i, b_i)$ where τ_i is the unknown time-delay and b_i accounts for the unknown Doppler stretch and, for, $n \in [0, N-1]$, $\mathbf{x}^T = (\ldots,\ x(nT_s),\ \ldots)$, $\mathbf{A}(\boldsymbol{\eta}_0, \boldsymbol{\eta}_1) = [\mathbf{a}_0,\ \mathbf{a}_1]$. $\mathbf{a}_i^T = \left(\ldots,\ s(nT_s - \tau_i)e^{-j\omega_c b_i (nT_s - \tau_i)}\ \ldots\right)$ is the time-delayed and frequency-shifted replica of the transmitted signal $s(nT_s)$. $\mathbf{w}^T = (\ldots,\ w(nT_s),\ \ldots)$ is the noise and $\boldsymbol{\alpha}^T = \left(\rho_0 e^{j\phi_0},\ \rho_1 e^{j\phi_1}\right)$ gathers the complex amplitudes of each path.

2.2. Close-to-Ground Assumptions

The receiver R being close to the ground (tens of meters above the reflecting surface), the relative path difference $\Delta\tau = \tau_1 - \tau_0$ is of the same order. Based on the link between height and path separation: $h = \frac{c\Delta\tau}{2\sin(e)}$ [13], the variation of the path separation with the transmitting satellite can be found in Fig. B.2 for the case $h = 25$m. From Fig. B.2, it is clear that both direct and reflected paths are very close in time. For most of the GNSS signals, even the recent GPS L5 and GALILEO E5A or E5B, a strong interference will exist. This contribution focuses on GPS L1 C/A signals but can be extended to the L5 band.

On the other hand, given the geometry and the motionless nature of the reflecting surface, the Doppler frequencies of both direct and reflected signals do not differ more than a fraction of Hertz. It can be shown that in a static geometry, the Doppler frequency difference between the direct signal and its reflection is only due to the receiver height and the elevation of the satellite. Indeed, for very low altitude scenarios, the phase difference between direct and reflected paths can be expressed as follows [14]: $\Delta\phi = \phi_1 - \phi_0 = \frac{2\omega_c h}{c}\sin(e)$. Then, as the satellite elevation e varies, the relative phase varies and the first derivative corresponds to the relative Doppler frequency: $\Delta F_d = (b_1 - b_0)f_c = \frac{2f_c h}{c}\cos(e)\frac{\mathrm{d}e}{\mathrm{d}t}$. This expression is often used for altimetry based on the SNR observations [1, 5] in GNSS-IR. A worst-case numerical application yields, for GPS L1 satellites with elevation rate $\mathrm{d}e/\mathrm{d}t = 0.14$ mrad/s, $e = 0$ rad, $f_c = 1575.42$ MHz and a receiver at altitude $h = 25$ m: $\Delta F_d \approx 0.04$ Hz. Such a small difference will not be observable for the coherent integration time considered in this study. In short, two main assumptions are made due to the considered low altitude geometry of the receiver: i) the Doppler frequencies of the direct and reflected paths are considered equal: $b_0 = b_1 = b$, and ii) the reflected path delay is very close to the direct delay $\tau_1 = \tau_0 + \Delta\tau$, $\Delta\tau$ small.

Consequently, $\boldsymbol{\eta}_0 = [\tau_0, b]^T$ and $\boldsymbol{\eta}_1 = [\tau_0 + \Delta\tau, b]^T$, and the final dual source CSM is given by:

$$\mathbf{x} = \mathbf{A}(\tau_0, \Delta\tau, b)\boldsymbol{\alpha} + \mathbf{w},\ \mathbf{w} \sim \mathcal{CN}(0, \sigma_n^2 \mathbf{I}_N)\ , \tag{2}$$

with, for $n \in [N_1, N_2]$, $\mathbf{A}(\tau_0, \Delta\tau, b) = [\mathbf{a}_0,\ \mathbf{a}_1]$, $\mathbf{a}_0$ previously defined in the dual source CSM, and $\mathbf{a}_1^T = \left(\dots,\ s(nT_s - \tau_0 - \Delta\tau)e^{-j\omega_c b(nT_s - \tau_0 - \Delta\tau)},\ \dots\right)$.

3. Approximate Maximum Likelihood Estimator

3.1. Dual Source Maximum Likelihood Estimator

Given the dual source CSM (2), the 2S-MLE of $\boldsymbol{\xi} \triangleq (\tau_0, \Delta\tau, b, \rho_0, \phi_0, \rho_1, \phi_1)^T$ is given by [15, 16]:

$$\left(\widehat{\tau_0}, \widehat{\Delta\tau}, \widehat{b}\right) = \arg\max_{\tau_0, \Delta\tau, b} \left\|\mathbf{P}_\mathbf{A}\mathbf{x}\right\|^2, \tag{3}$$

and, for $(\tau_0, \Delta\tau, b) = \left(\widehat{\tau_0}, \widehat{\Delta\tau}, \widehat{b}\right)$ and $i \in \{0, 1\}$, $\widehat{\rho_i} = \left|\left[\left(\mathbf{A}^H\mathbf{A}\right)^{-1}\mathbf{A}^H\mathbf{x}\right]_i\right|$, $\widehat{\phi_i} = \arg\left\{\left[\left(\mathbf{A}^H\mathbf{A}\right)^{-1}\mathbf{A}^H\mathbf{x}\right]_i\right\}$, $\widehat{\sigma_n^2} = \frac{1}{N}\left\|\mathbf{P}_\mathbf{A}^\perp\mathbf{x}\right\|^2$, where $\mathbf{P}_\mathbf{A} = \mathbf{A}\left(\mathbf{A}^H\mathbf{A}\right)^{-1}\mathbf{A}^H$ is the projection matrix onto the subspace spanned by the columns of $\mathbf{A}$ (signal subspace) and $\mathbf{P}_\mathbf{A}^\perp = \mathbf{I} - \mathbf{P}_\mathbf{A}$ is the projection matrix onto the noise subspace where the relationships with τ_0, b and $\Delta\tau$ are omitted for the sake of readability.

3.2. Approximation of the Maximum Likelihood Criterion

As stated in (3), the 2S-MLE requires a computationally expensive maximization over a three-dimensional parameter space. The aim of this contribution is to adapt the AMLE presented in [6] for spectral analysis to the problem of time-delay estimation to reduce the computational burden.

The likelihood criterion, noted $L(\tau_0, \Delta\tau, b)$ to be maximized and defined in (3) can be written as follows: $L(\tau_0, \Delta\tau, b) \triangleq \left\|\mathbf{P}_\mathbf{A}\mathbf{x}\right\|^2 = \mathbf{x}^H\mathbf{P}_\mathbf{A}\mathbf{x} = \left(\mathbf{A}^H\mathbf{x}\right)^H\left(\mathbf{A}^H\mathbf{A}\right)^{-1}\mathbf{A}^H\mathbf{x}$, where the inverse matrix can be explicitly written with respect to (w.r.t.) the path separation $\Delta\tau$: $\left(\mathbf{A}^H\mathbf{A}\right)^{-1} \propto \frac{1}{1-|c(\Delta\tau)|^2}\begin{bmatrix} 1 & -c(\Delta\tau) \\ -c(\Delta\tau)^* & 1 \end{bmatrix}$, with $c(\Delta\tau) \propto \mathbf{a}_0^H\mathbf{a}_1$ the auto-correlation of the signal expressed in $\Delta\tau$. Now if one expands the matrices product, the projector $\mathbf{P}_\mathbf{A}$ results in a finite sum of similar terms: $\mathbf{P}_\mathbf{A} = \frac{\mathbf{a}_0\mathbf{a}_0^H + \mathbf{a}_1\mathbf{a}_1^H - c(\Delta\tau)^*\mathbf{a}_0\mathbf{a}_1^H - c(\Delta\tau)\mathbf{a}_1\mathbf{a}_0^H}{1-|c(\Delta\tau)|^2}$, and, with, for $i \in \{0, 1\}$, $\beta_i = \mathbf{a}_i^H\mathbf{x}$, the likelihood criterion can be expressed as

$$L(\tau_0, \Delta\tau, b) = \frac{\beta_0^*\beta_0 + \beta_1^*\beta_1 - c(\Delta\tau)^*\beta_0^*\beta_1 - c(\Delta\tau)\beta_1^*\beta_0}{1 - |c(\Delta\tau)|^2}. \tag{4}$$

Expression (4) can be further simplified by exploiting the fact that $\Delta\tau$ is very small. In that case both $c(\Delta\tau)$ and β_1 can be approximated with a truncation of their Taylor series: $c(\Delta\tau) = 1 + \sum_{n\in\mathbb{N}^*} c_n\Delta\tau^n$, $|c(\Delta\tau)|^2 = 1 + \sum_{n\in\mathbb{N}^*} d_n\Delta\tau^n$, $\beta_1 = \beta_0 + \sum_{n\in\mathbb{N}^*} \beta_{1,n}\Delta\tau^n$, where c_n, d_n and $\beta_{1,n}$ are the n-th Taylor coefficients of $c(\Delta\tau)$, $|c(\Delta\tau)|^2$ and β_1, respectively.

Proof. see Appendix A. ∎

By truncating and expanding theses series, it is possible to obtain a 3rd order Taylor development:

$$L(\tau_0, \Delta\tau, b) \approx L^{\text{Taylor}}(\tau_0, \Delta\tau, b) = \sum_{n=0}^{3} L_n(\tau_0, b)\Delta\tau^n \tag{5}$$

with $L_0(\tau_0, b) = -\frac{B_2}{d_2}$, $L_1(\tau_0, b) = -\frac{B_3}{d_2}$, $L_2(\tau_0, b) = -\frac{1}{d_2}\left(B_4 - \frac{d_4}{d_2}B_2\right)$, $L_3(\tau_0, b) = -\frac{1}{d_2}\left(B_5 - \frac{d_4}{d_2}B_3\right)$, and B_n and d_n can be expressed w.r.t. the baseband signal samples thanks to (A.4) and (A.7).

Proof. see Appendix B. ∎

3.3. Description of the Algorithm

3.3.1. Intuition

In (5), the dependency on the relative delay $\Delta\tau$ is simplified. To better illustrate the meaning of this approximation, one can plot the real likelihood criterion $L(\tau_0, \Delta\tau, b)$ and compare it to its different order Taylor approximations. In Fig. B.3, a cut at the true values of τ_0 and b of the exact likelihood function is displayed along with the corresponding Taylor approximations (from order 0 to 3). These figures are two illustrations without noise, for a signal GPS L1 C/A with F_s = 4 MHz, b = 0, ρ_1/ρ_0 = 0.5 and $\Delta\phi = \phi_1 - \phi_0 = 0$. The only difference between the two figures is the relative delay which is small in Fig. B.3a and larger in Fig. B.3b. From these figures, it is clear that the order of the Taylor approximation is important: for very small $\Delta\tau$ (Fig. B.3a), the likelihood is well represented at the 2nd order around the extremum area, which is of interest since the criterion is maximized for the correct value of $\Delta\tau$. In the case of a larger $\Delta\tau$ (Fig. B.3b), the 2nd order is not fitting the true likelihood function around the extremum anymore. On the other hand, the 3rd order provides a good approximation. The true likelihood function maximum being approximated by one of the two extrema of the 3rd order polynomial.

3.3.2. Resolution of the 3rd order polynomial

To obtain an estimation of $\Delta\tau$, one wants then to maximize the likelihood criterion. The observations made from Fig. B.3 suggest to relate the maximum of the likelihood function to one of the extrema of the 3rd order Taylor approximation. These extrema can be obtained by zeroing the first derivative of (5). Then, the correct extremum is the one that has a negative second derivative. Consequently, to obtain a closed form of $\widehat{\Delta\tau}$ from (5), one can do as follows: i) Find the two closed form candidates $\Delta\tau_1$ and $\Delta\tau_2$ by zeroing the first derivative of (5) and ii) pick the candidate that has a negative curvature.

3.3.3. Wrap-up of the algorithm

To sum up, the 3rd order Taylor approximation of the likelihood function allows to find a closed-form solution for the estimated relative delay $\widehat{\Delta\tau}$ for all τ_0 and b. Once the procedure presented in the previous

paragraph is done, one can inject $\widehat{\Delta\tau}$ in the Taylor approximation of the likelihood function (5). The MLE (3) turns to an AMLE defined by

$$(\widehat{\tau_0}, \widehat{b}) = \arg\min_{\tau_0, b} \left(L^{\text{Taylor}}(\tau_0, \widehat{\Delta\tau}(\tau_0, b), b) \right). \tag{6}$$

The proposed AMLE is summarized in the Algorithm 1.

In terms of complexity, the 2S-MLE, presented in (3), is a three-dimensional maximization problem. The AMLE reduces this to a two-dimensional problem which is similar to a single source MLE.

3.4. Discussion on the Approximation Validity

Based on Appendix A, the AMLE cannot be expected to perform well when the path separation is too important. Consequently, it is necessary to study the goodness-of-fit between the auto-correlation function $c(\tau)$ and its 4^{th} order Taylor approximation involved in the approximation of the likelihood function. Fig. B.4 presents the exact and 4^{th} order Taylor approximation of the auto-correlation of a GPS L1 C/A signal, sampled at different values of the sampling frequency F_s. Comparing different values of F_s here is similar to comparing different qualities of receivers where the baseband signal has been sampled at a frequency equal to the RF front-end bandwidth. In this figure, the effect of F_s on the resulting shape of the exact auto-correlation function is clearly visible: the larger F_s, the more oscillations along the slopes one will observe. It is not surprising that the Taylor approximation is sensitive to these oscillations since they are impossible to model with a 4^{th} order polynomial. Consequently, the Taylor approximation will be valid for a larger range of time delays around 0 when the signal will have a smaller bandwidth.

4. Performance on Simulated Data

4.1. Simulation Set-Up

To look at the performance of the AMLE, the MSE of the estimated path separation is compared to the MSE of the 2S-MLE defined in Sec. 3.1. The estimation performance of the signal time-delay τ_0 is also investigated with a comparison between the AMLE, the 2S-MLE and a standard single source processing. A GPS L1 C/A signal is considered with RF front-end bandwidth set to 4 MHz. The path separation considered is set to 0.085 C/A chips, two phase differences are considered: $\Delta\phi = \pi/3$ and $\Delta\phi = 2\pi/3$, and the relative amplitude is set to 0.5. Considering the model approximations, the AMLE does not look at $\Delta\tau$ candidates greater than 0.25 C/A chips, consequently, the RMSE is upper bounded, which may lead to RMSE smaller than the CRB at low SNRno. In order to fairly compare the AMLE and the 2S-MLE performance, the same restriction has been applied to the 2S-MLE. Each point is estimated with 2000 Monte Carlo simulations.

4.2. Cramér-Rao Bounds

From the joint delay-Doppler estimation problem for the estimation of $\boldsymbol{\epsilon}^T = (\sigma_n^2, \boldsymbol{\eta}_0, \rho_0, \phi_0, \boldsymbol{\eta}_1, \rho_1, \phi_1)$ presented in [12], and its corresponding Fisher Information Matrix (FIM) $\mathbf{F}_{\boldsymbol{\epsilon}|\boldsymbol{\epsilon}}$, it is straightforward to obtain an expression of the FIM for the vector of parameters under study $\boldsymbol{\xi}^T = (\sigma_n^2, \tau_0, \Delta\tau, b, \rho_0, \phi_0, \rho_1, \phi_1)$ using $\mathbf{F}_{\boldsymbol{\xi}|\boldsymbol{\xi}} = \left(\frac{\partial \boldsymbol{\epsilon}}{\partial \boldsymbol{\xi}^T}\right)^T \mathbf{F}_{\boldsymbol{\epsilon}|\boldsymbol{\epsilon}} \frac{\partial \boldsymbol{\epsilon}}{\partial \boldsymbol{\xi}^T}$, where $\frac{\partial \boldsymbol{\epsilon}}{\partial \boldsymbol{\xi}^T}$ is the Jacobian of the application for which the image of $\boldsymbol{\xi}$ is $\boldsymbol{\epsilon}$, defined by the constraints derived from the close-to-ground assumptions enumerated in Sec. 2.2: $b_0 = b_1 = b$ and $\Delta\tau = \tau_1 - \tau_0$. The CRB for the estimation of $\boldsymbol{\xi}$ is the inverse of the resulting FIM.

4.3. Results

Fig. B.5 presents the root MSE (RMSE) of both AMLE and 2S-MLE for the estimation of the path separation. For both relative phase $\Delta\phi$, the performance of the proposed algorithm AMLE and the 2S-MLE are similar over a wide range of SNR. This is true up to a certain SNR point (about 42 dB) where the bias induced by the Taylor approximation becomes larger than the standard deviation. The AMLE approach seems a promising solution for scenarios with a SNR that ranges from 30 dB to 42 dB.

Another result is shown in Fig. B.6, where the RMSE of the AMLE, the 2S-MLE and the 1S-MLE for the estimation of the main signal time-delay are compared. As expected for the single source processing, the bias induced by the misspecification appears at a given SNR level [17]. Again the AMLE and the 2S-MLE present very similar performance and one can notice that the bias induced by the Taylor approximation visible in Fig. B.5 does not appear for the estimation of the direct signal time-delay. This suggests that the AMLE can be used as a multipath mitigation technique for robust navigation applications.

5. Conclusion

In this paper, an estimator based on the 3$^{\text{rd}}$ order Taylor approximation of the likelihood criterion has been presented for the time-delay estimation of two closely spaced sources. It is of particular interest in ground-based GNSS-R where a direct signal and its reflection from a reflecting surface impinges a receiver antenna. To illustrate this approximate MLE, a few scenarios have been selected and simulations were run in order to compare its MSE to the exact 2S-MLE and the corresponding CRB for the estimation of the path separation. Results show that the proposed AMLE and the 2S-MLE have similar performance for a large range of SNR. The AMLE performance for the estimation of the main signal was also compared to the 2S-MLE and a misspecified 1S-MLE. A key result from this study is that the AMLE turns out to be a good candidate for multipath mitigation, again providing a performance equivalent to the 2S-MLE.

Acknowledgment

This work was partially supported by the DGA/AID projects 2022.65.0082 and 2021.65.0070.00.470.75.01 and CNES.

Appendix A. Details on the Taylor Approximation of c and β_1 Functions

Appendix A.1. Auto-correlation Function

From the discrete signal model, if the number of elements $N_2 - N_1$ is very large, the auto-correlation function $c(\Delta\tau)$ can be written as an integral: $c(\Delta\tau) = \mathbf{a}_0^H \mathbf{a}_1 = F_s \int_{\mathbb{R}} s(t-\tau_0)^* s(t-\tau_0-\Delta\tau) e^{j\omega_c b\Delta\tau} \mathrm{d}t = F_s e^{j\omega_c b\Delta\tau} \int_{\mathbb{R}} s(u)^* s(u-\Delta\tau)\mathrm{d}u$. Then using the Fourier transform properties over the hermitian product and the sum definition of the Fourier transform:

$$c(\Delta\tau) = F_s e^{j\omega_c b\Delta\tau} \int_{-F_s/2}^{F_s/2} \left(\frac{1}{F_s} \sum_{n=N_1}^{N_2} s(nT_s) e^{-j2\pi f nT_s} \right)^* \left(\frac{1}{F_s} \sum_{n=N_1}^{N_2} s(nT_s) e^{-j2\pi f nT_s} \right) e^{-j2\pi f \Delta\tau} \mathrm{d}f \tag{A.1}$$

$$= \mathbf{s}^H \left(\int_{-1/2}^{1/2} \boldsymbol{\nu}(f)\boldsymbol{\nu}(f)^H e^{-j2\pi f F_s \Delta\tau} \mathrm{d}f \right) \mathbf{s}\, e^{j\omega_c b\Delta\tau} \tag{A.2}$$

where, for $n \in [N_1, N_2]$, $\mathbf{s} = (\ldots,\ s(nT_s),\ \ldots)^T$, $\boldsymbol{\nu}(f) = (\ldots,\ e^{j2\pi f n},\ \ldots)^T$. Consequently, the Fourier coefficients for the auto-correlation function are the successive derivatives of (A.2) evaluated when $\Delta\tau = 0$:

$$c_n = \frac{1}{n!} \left. \frac{\partial^n c(\Delta\tau)}{\partial \Delta\tau^n} \right|_{\Delta\tau=0} = \frac{1}{n!} \sum_{k=0}^{n} \mathbf{s}^H \mathbf{D}_k(0) \mathbf{s} (j\omega_c b)^{n-k}, \text{ where } \mathbf{D}_k(\tau) = (-j2\pi F_s)^k \int_{-1/2}^{1/2} f^k \boldsymbol{\nu}(f)\boldsymbol{\nu}(f)^H e^{-j2\pi f \tau} \mathrm{d}f. \tag{A.3}$$

When expressed with $\tau = 0$, $\mathbf{D}_k(0)$ is the k^{th} derivative of a sine cardinal function which can be iteratively computed (see Appendix A.3). If $\Delta\tau$ is very small, the Taylor series for the auto-correlation term is:

$$c(\Delta\tau) = \sum_{n\in\mathbb{N}} c_n \Delta\tau^n = 1 + \sum_{n\in\mathbb{N}^*} c_n \Delta\tau^n \text{ and } |c(\Delta\tau)|^2 = \sum_{n\in\mathbb{N}} \left(\sum_{k=0}^{n} c_k c_{n-k}^* \right) \Delta\tau^n = 1 + \sum_{n\in\mathbb{N}^*} d_n \Delta\tau^n. \tag{A.4}$$

Appendix A.2. Cross-correlation Function

Similarly, when the number of element is large enough, the cross-correlation between $\mathbf{a}_1$ and the data $\mathbf{x}$ can be expressed as $\beta_1 = \mathbf{a}_1^H \mathbf{x} = F_s \int_{\mathbb{R}} \left(s(t-\tau_0-\Delta\tau) e^{-j2\pi f_c b(t-\tau_0-\Delta\tau)} \right)^* x(t)\mathrm{d}t$. In the frequency domain,

$$\beta_1 = F_s \int_{-F_s/2}^{F_s/2} \left(\frac{1}{F_s} \sum_{n=N_1}^{N_2} s(nT_s) e^{-j2\pi(f+f_c b)nT_s} \right)^* \left(\frac{1}{F_s} \sum_{n=N_1}^{N_2} x(nT_s) e^{-j2\pi f nT_s} \right) e^{j2\pi f(\tau_0+\Delta\tau)} \mathrm{d}f \tag{A.5}$$

$$= \mathbf{s}^H \mathbf{U}^H \left(\frac{f_c b}{F_s} \right) \left(\int_{-1/2}^{1/2} \boldsymbol{\nu}(f)\boldsymbol{\nu}(f)^H e^{j2\pi f F_s(\tau_0+\Delta\tau)} \mathrm{d}f \right) \mathbf{x}, \tag{A.6}$$

where $\mathbf{U}(b) = \mathrm{diag}\left(\ldots,\ e^{-j2\pi bn},\ \ldots\right)_{N_1 \le n \le N_2}$. Then the Taylor series for the cross-correlation term is deduced from the successive derivatives of (A.6):

$$\beta_{1,k} = \frac{1}{k!} \left. \frac{\partial^k \beta_1}{\partial \Delta\tau^k} \right|_{\Delta\tau=0} = \frac{1}{k!} \left(\mathbf{D}_k \left(\frac{\tau_0}{T_s} \right) \mathbf{U} \left(\frac{f_c b}{F_s} \right) \mathbf{s} \right)^H \mathbf{x} = \frac{1}{k!} R^{(k)}_{\mathbf{x},\mathbf{D}\mathbf{s}}(\tau_0, b f_c). \tag{A.7}$$

The term $R^{(k)}_{\mathbf{x},\mathbf{Ds}}(\tau_0, bf_c)$ is actually the cross-correlation between the data $\mathbf{x}$ and the k^{th} derivative of the signal $\mathbf{s}$. Similarly to the auto-correlation term, it is expressed w.r.t. the successive derivatives of a sine cardinal which can be iteratively computed as detailed in Appendix A.3. Therefore, for small values of $\Delta\tau$, the Taylor series for the cross-correlation term is: $\beta_1 = \sum_{n\in\mathbb{N}} \beta_{1,n}\Delta\tau^n = \beta_0 + \sum_{n\in\mathbb{N}^*} \beta_{1,n}\Delta\tau^n$.

Appendix A.3. Note on the Sine Cardinal Derivatives

The Taylor coefficients derived in the previous section all depend on the successive derivatives of a sine cardinal of the form: $\text{sinc}(u-\delta u) = \int_{-1/2}^{1/2} e^{j2\pi f(u-\delta u)}\mathrm{d}f$. If one calculates the k^{th} derivative of this expression, $\frac{\partial^k \text{sinc}(u-\delta u)}{\partial \delta u^k} = (-j2\pi)^k \int_{-1/2}^{1/2} f^k e^{j2\pi f(u-\delta u)}\mathrm{d}f$, a first integration by parts yields

$$\frac{\partial^k \text{sinc}(u-\delta u)}{\partial \delta u^k} = (-j2\pi)^k \left[\frac{f^k e^{j2\pi f(u-\delta u)}}{j2\pi(u-\delta u)}\right]_{-1/2}^{1/2} - \frac{k(-j2\pi)^k}{j2\pi(u-\delta u)} \int_{-1/2}^{1/2} f^{k-1} e^{j2\pi f(u-\delta u)}\mathrm{d}f \tag{A.8}$$

$$= \frac{(-j2\pi)^k}{j2\pi(u-\delta u)} \left(\left(\frac{1}{2}\right)^k e^{j\pi(u-\delta u)} - \left(-\frac{1}{2}\right)^k e^{-j\pi(u-\delta u)}\right) + \frac{k}{u-\delta u}\frac{\partial^{k-1}\text{sinc}(u-\delta u)}{\partial \delta u^{k-1}}. \tag{A.9}$$

Then, depending on the parity of k, an iterative expression of the sine cardinal derivatives can be obtained:

$$\frac{\partial^{2n}\text{sinc}(u-\delta u)}{\partial \delta u^{2n}} = \frac{2n}{u-\delta u}\frac{\partial^{2n-1}\text{sinc}(u-\delta u)}{\partial \delta u^{2n-1}} + (-1)^n \pi^{2n}\text{sinc}(u-\delta u)\ ,\ \text{for } k = 2n, \tag{A.10}$$

$$\frac{\partial^{2n+1}\text{sinc}(u-\delta u)}{\partial \delta u^{2n+1}} = \frac{2n+1}{u-\delta u}\frac{\partial^{2n}\text{sinc}(u-\delta u)}{\partial \delta u^{2n}} + (-1)^{n+1} \pi^{2n+1}\frac{\cos(\pi(u-\delta u))}{\pi(u-\delta u)}\ ,\ \text{for } k = 2n+1. \tag{A.11}$$

Appendix B. Details on the Taylor Approximation of the Likelihood Criterion

Starting from (4), reminded here, $L(\tau_0, \Delta\tau, b) = \frac{\beta_0^*\beta_0 + \beta_1^*\beta_1 - c(\Delta\tau)^*\beta_0^*\beta_1 - c(\Delta\tau)\beta_1^*\beta_0}{1-|c(\Delta\tau)|^2}$, each term can be expressed as a Taylor series:

$$\beta_1^*\beta_1 = \beta_0^*\beta_0 + \sum_{n\in\mathbb{N}^*}\left(\sum_{k=0}^{n}\beta_{1,k}^*\beta_{1,n-k}\right)\Delta\tau^n\ ,\ c(\Delta\tau)^*\beta_0^*\beta_1 = \beta_0^*\beta_0 + \sum_{n\in\mathbb{N}^*}\left(\sum_{k=0}^{n} c_k^*\beta_0^*\beta_{1,n-k}\right)\Delta\tau^n \tag{B.1}$$

$$c(\Delta\tau)\beta_1^*\beta_0 = \beta_0^*\beta_0 + \sum_{n\in\mathbb{N}^*}\left(\sum_{k=0}^{n} c_k\beta_{1,n-k}^*\beta_0\right)\Delta\tau^n\ ,\ 1-|c(\Delta\tau)|^2 = -\sum_{n\in\mathbb{N}^*} d_n\Delta\tau^n. \tag{B.2}$$

Then, by reordering these terms, the likelihood criterion can be written as follows:

$$L(\tau_0, \Delta\tau, b) = -\frac{\sum_{n\in\mathbb{N}^*} B_n\Delta\tau^{n-1}}{\sum_{n\in\mathbb{N}^*} d_n\Delta\tau^{n-1}} \text{ with } B_n \triangleq \sum_{k=0}^{n}\beta_{1,k}^*\beta_{1,n-k} - c_k^*\beta_0^*\beta_{1,n-k} - c_k\beta_{1,n-k}^*\beta_0. \tag{B.3}$$

The auto-correlation function Taylor coefficients, expressed with the derivatives of the sine cardinal present a number of symmetries that simplify the expression of B_n and d_n: with $c_1^* = -c_1$, $c_3^* = -c_3$, one can deduce $d_1 = d_3 = 0$ and similarly $B_1 = 0$. Consequently, if the Taylor series in (B.3) are truncated to the

3^{rd} order, the likelihood criterion reduces to $L(\tau_0, \Delta\tau, b) \approx -\frac{B_2+B_3\Delta\tau+B_4\Delta\tau^2+B_5\Delta\tau^3}{d_2+d_4\Delta\tau^2}$. Finally, using the series representation of the denominator, the criterion can be written as a 3^{rd} order Taylor expansion as in

$$\frac{-1}{d_2 + d_4\Delta\tau^2} \approx -\frac{1}{d_2}\left(1 - \frac{d_4}{d_2}\Delta\tau^2\right) \Rightarrow L(\tau_0, \Delta\tau, b) \approx L^{\text{Taylor}}(\tau_0, \Delta\tau, b) = \sum_{n=0}^{3} L_n(\tau_0, b)\Delta\tau^n, \tag{B.4}$$

with $L_0(\tau_0, b) = -\frac{B_2}{d_2}$, $L_1(\tau_0, b) = -\frac{B_3}{d_2}$, $L_2(\tau_0, b) = -\frac{1}{d_2}\left(B_4 - \frac{d_4}{d_2}B_2\right)$, $L_3(\tau_0, b) = -\frac{1}{d_2}\left(B_5 - \frac{d_4}{d_2}B_3\right)$.

References

[1] K. M. Larson, E. E. Small, E. D. Gutmann, A. L. Bilich, J. J. Braun, V. U. Zavorotny, Use of GPS Receivers as a Soil Moisture Network for Water Cycle Studies, Geophysical Research Letters 35 (24).

[2] M. Durand, A. Rivera, F. Geremia-Nievinski, M. G. Lenzano, J. F. G. Monico, P. Paredes, L. Lenzano, GPS Reflectometry Study Detecting Snow Height Changes in the Southern Patagonia Icefield, Cold Regions Science and Technology 166 (2019) 102840.

[3] P. Zeiger, F. Frappart, J. Darrozes, N. Roussel, P. Bonneton, N. Bonneton, G. Detandt, SNR-Based Water Height Retrieval in Rivers: Application to High Amplitude Asymmetric Tides in the Garonne River, Remote Sensing 13 (9). doi:10.3390/rs13091856.

[4] L. Lestarquit, M. Peyrezabes, J. Darrozes, E. Motte, N. Roussel, G. Wautelet, F. Frappart, G. Ramillien, R. Biancale, M. Zribi, Reflectometry With an Open-Source Software GNSS Receiver: Use Case With Carrier Phase Altimetry, IEEE Journal of Selected Topics in Applied Earth Observations and Remote Sensing 9 (10) (2016) 4843–4853.

[5] M. A. Ribot, J.-C. Kucwaj, C. Botteron, S. Reboul, G. Stienne, J. Leclère, J.-B. Choquel, P.-A. Farine, M. Benjelloun, Normalized GNSS Interference Pattern Technique for Altimetry, Sensors 14 (6) (2014) 10234–10257. doi:10.3390/s140610234.

[6] F. Vincent, O. Besson, E. Chaumette, Approximate Maximum Likelihood Estimation of Two Closely Spaced Sources, Signal Processing 97 (2014) 83–90. doi:10.1016/j.sigpro.2013.10.017.

[7] P. Heidenreich, A. M. Zoubir, Fast Maximum Likelihood DOA Estimation in the Two-Target Case with Applications to Automotive Radar, Signal Processing 93 (12) (2013) 3400–3409.

[8] Y. Zhang, Y. Jin, Y. Wu, C. Hao, D. Orlando, Sparsity-Based Time Delay Estimation Through the Matched Filter Outputs, IEEE Signal Processing Letters 29 (2022) 1769–1773. doi:10.1109/LSP.2022.3195427.

[9] Q. Song, X. Ma, High-Resolution Time Delay Estimation Algorithms Through Cross-Correlation Post-Processing, IEEE Signal Processing Letters 28 (2021) 479–483. doi:10.1109/LSP.2020.3048843.

[10] M. Haardt, F. Roemer, G. Del Galdo, Higher-Order SVD-Based Subspace Estimation to Improve the Parameter Estimation Accuracy in Multidimensional Harmonic Retrieval Problems, IEEE Transactions on Signal Processing 56 (7) (2008) 3198–3213.

[11] D. V. de Lima, M. da Rosa Zanatta, J. P. C. L. da Costa, R. T. de Sousa Jr, M. Haardt, Robust tensor-based techniques for antenna array-based GNSS receivers in scenarios with highly correlated multipath components, Digital Signal Processing 101 (102715) (2020) 1–15.

[12] C. Lubeigt, L. Ortega, J. Vilà-Valls, L. Lestarquit, E. Chaumette, Joint Delay-Doppler Estimation Performance in a Dual Source Context, Remote Sensing 12 (23) (2020) 3894. doi:10.3390/rs12233894.

[13] V. U. Zavorotny, S. Gleason, E. Cardellach, A. Camps, Tutorial on Remote Sensing Using GNSS Bistatic Radar of Opportunity, IEEE Geoscience and Remote Sensing Magazine 2 (4) (2014) 8–45.

[14] Y. Georgiadou, A. Kleusberg, On Carrier Signal Multipath Effects in Relative GPS Positioning, Manuscripta Geodaetica 13 (3) (1988) 172–179.

[15] P. Stoica, A. Nehorai, MUSIC, Maximum Likelihood, and Cramér-Rao Bound, IEEE Transactions on Acoustics, Speech, and Signal Processing 37 (5) (1989) 720–741. doi:10.1109/29.17564.

[16] B. Ottersten, M. Viberg, P. Stoica, A. Nehorai, Exact and Large Sample Maximum Likelihood Techniques for Parameter Estimation and Detection in Array Processing, in: S. Haykin, J. Litva, T. J. Shepherd (Eds.), Radar Array Processing, Springer-Verlag, Heidelberg, 1993, Ch. 4, pp. 99–151.

[17] C. Lubeigt, L. Ortega, J. Vilà-Valls, E. Chaumette, Untangling First and Second Order Statistics Contributions in Multipath Scenarios, Signal Processing 205 (2023) 108868. doi:https://doi.org/10.1016/j.sigpro.2022.108868.

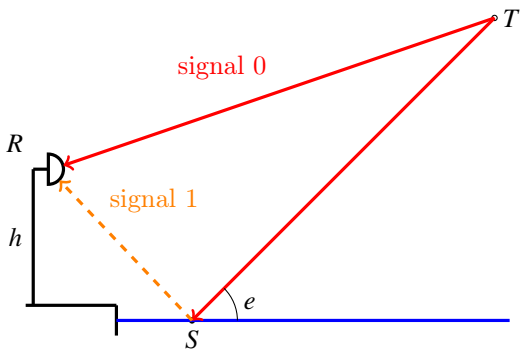

Figure B.1: GNSS-R geometry with the local elevation angle e of the transmitting satellite T and the height h of the receiver R.

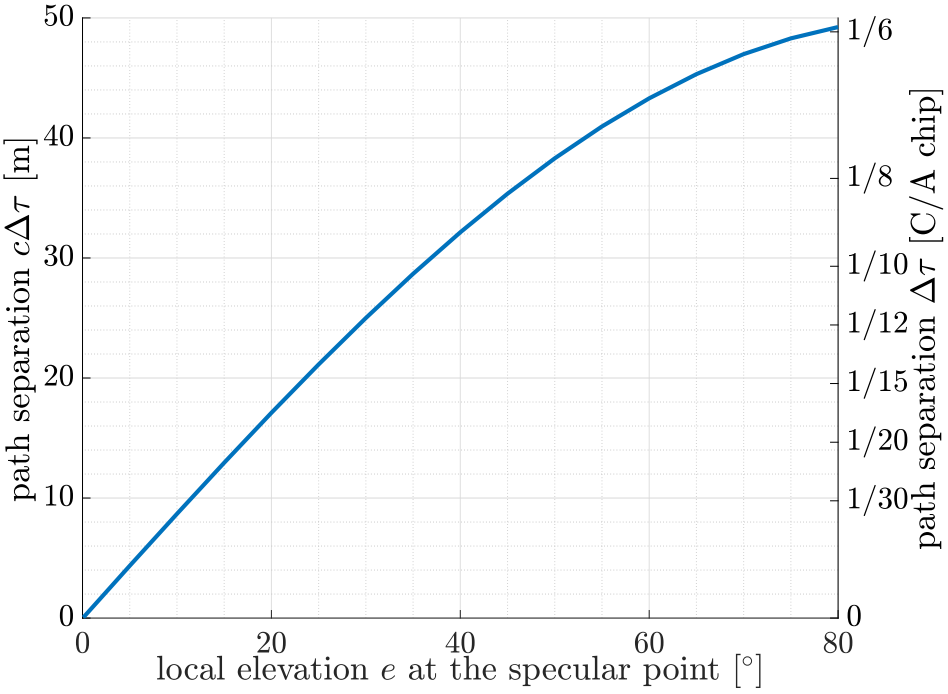

Figure B.2: Path separation evolution with regard to the local elevation e of the transmitting satellite for a receiver height $h = 25$m.

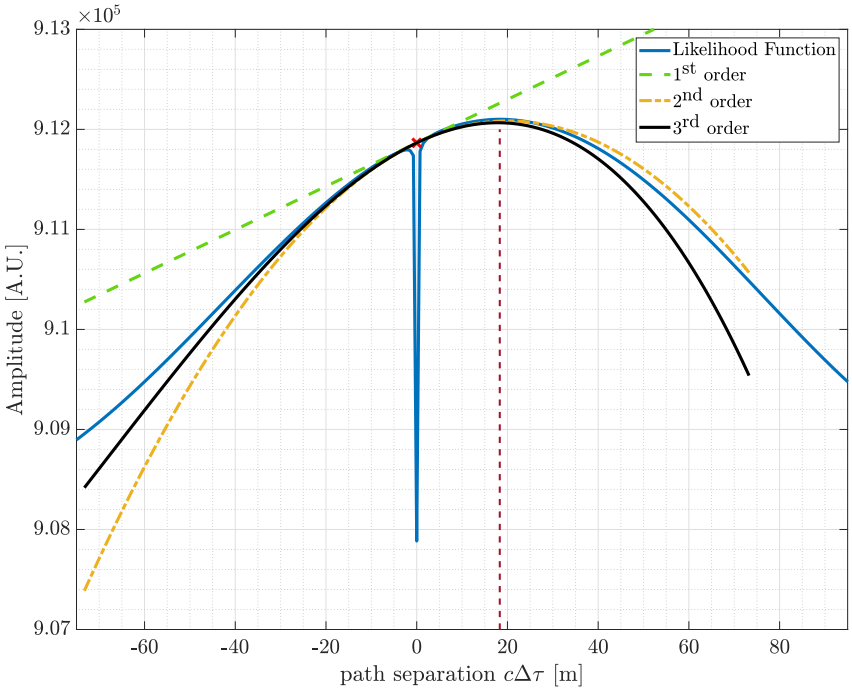

(**a**) $\Delta\tau$ = 1/16 L1 C/A chips (~ 18.31m).

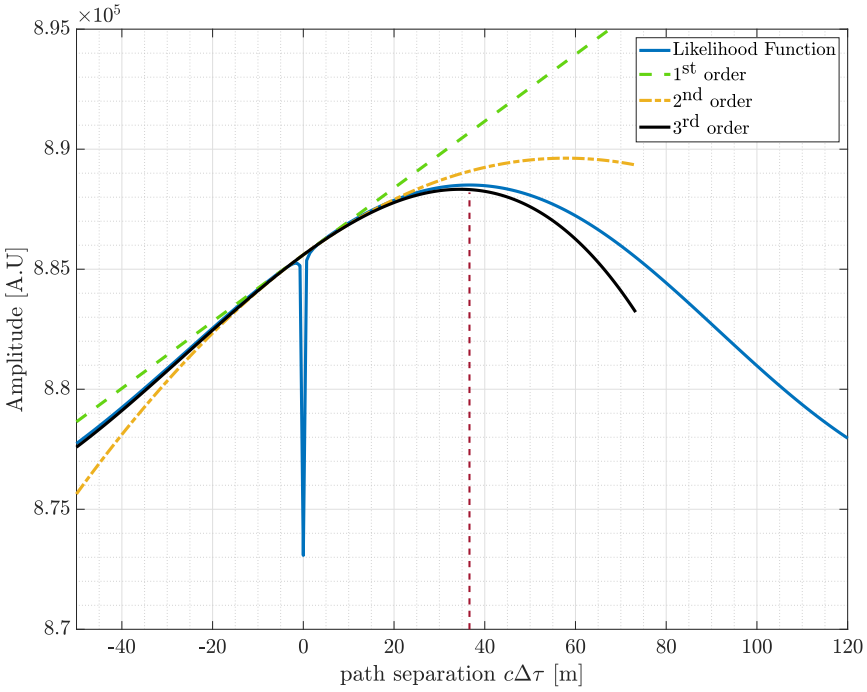

(**b**) $\Delta\tau$ = 1/8 L1 C/A chips (~ 32.63m).

Figure B.3: Illustration of the likelihood criterion Taylor approximations at different orders and relative delay $\Delta\tau$.

Algorithm 1: Approximate Maximum Likelihood estimator.

`// Clean replica Taylor coefficients. These can be computed before-hand, they do not depend on the data vector x.`

Compute $\mathbf{D}_n\mathbf{s}$ using (A.3) and Appendix A.3;

Compute c_n using (A.3) and d_n using (A.4);

`// Likelihood criterion Taylor approximation:`

Compute β_0 and $\beta_{1,n}$ using (A.7);

Compute B_n using (B.3);

Compute L_n using (5);

`// Polynomial solution to get` $\Delta\tau$ `for all` τ_0 `and` b`:`

$\Delta\tau_{1/2} = \frac{-L_2 \pm \sqrt{\delta}}{3L_3}$ with $\delta = L_2^2 - 3L_1L_3$; `//` δ `is the reduced discrimant.`

$\widehat{\Delta\tau}(\tau_0, b) = \arg\min_{\Delta\tau_1, \Delta\tau_2} (2L_2 + 6L_3\Delta\tau)$;

`// Reduced maximization problem:`

$(\widehat{\tau_0}, \widehat{b}) = \arg\min_{\tau_0, b} \left(L^{\text{Taylor}}(\tau_0, \widehat{\Delta\tau}(\tau_0, b), b) \right)$;

Evaluate $\widehat{\Delta\tau}(\widehat{\tau_0}, \widehat{b})$;

return $\widehat{\tau_0}$, $\widehat{\Delta\tau}$, $\widehat{b}$.

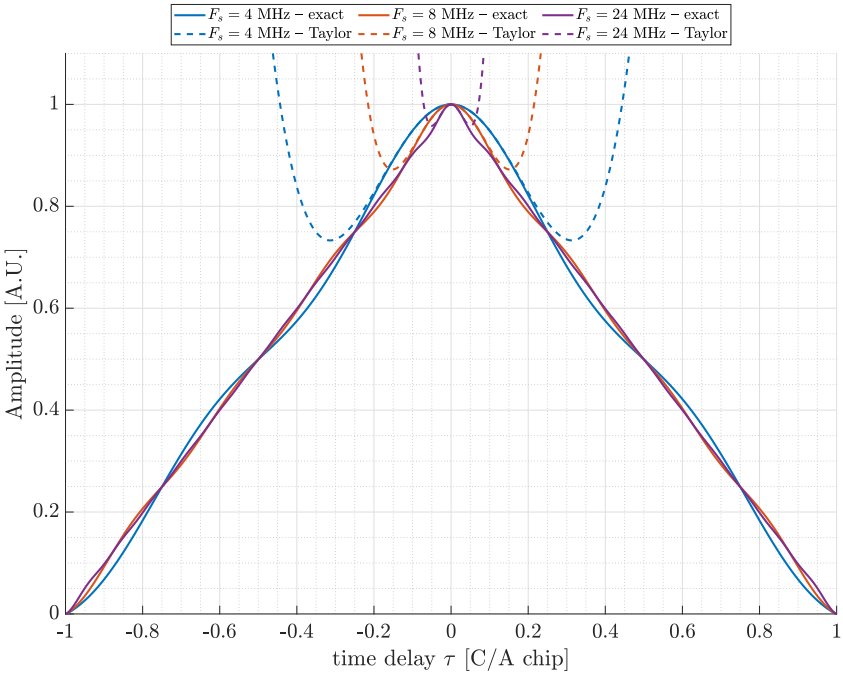

Figure B.4: Exact (plain lines) and 4^{th} order Taylor approximation (dashed lines) auto-correlation function for different sampling frequencies $F_s \in \{4, 8, 24\}$ MHz.

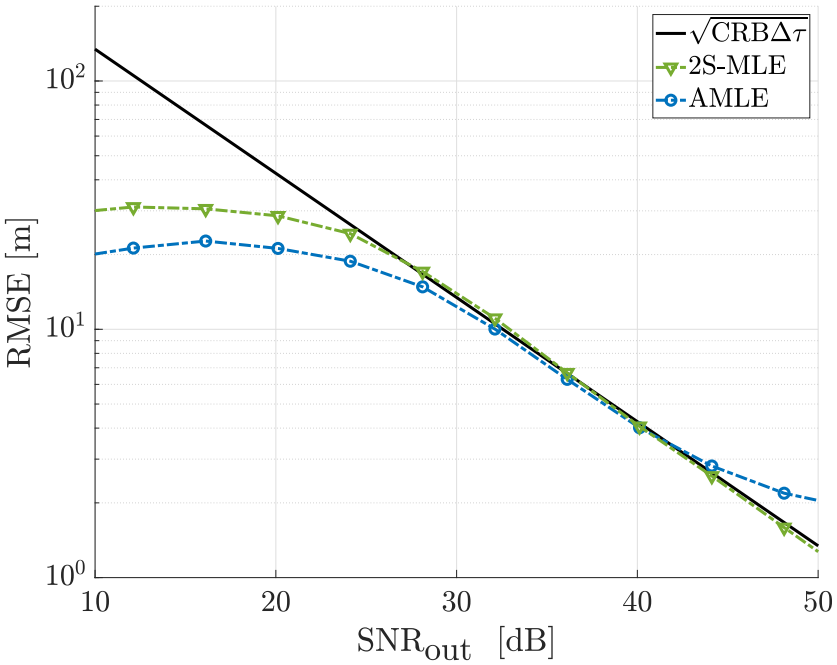

(**a**)

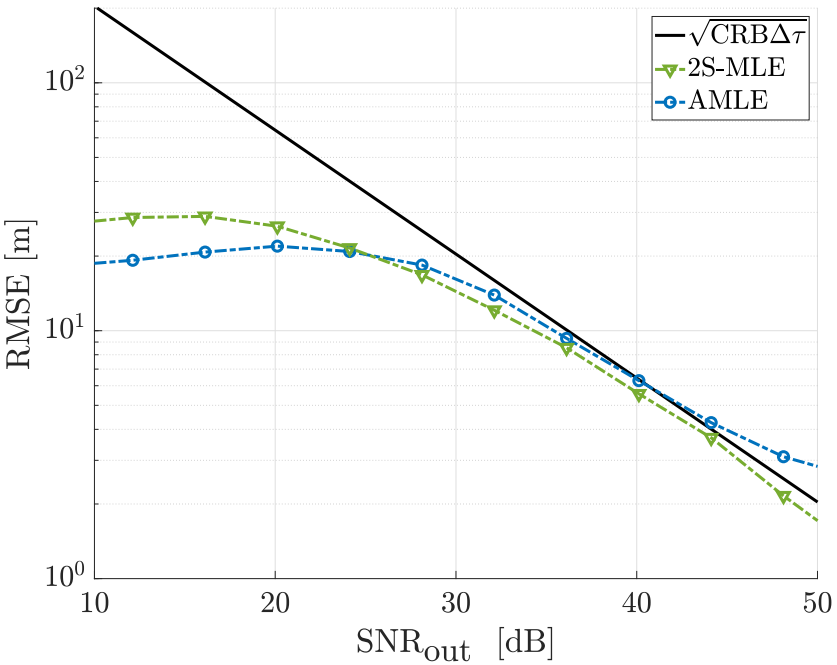

(**b**)

Figure B.5: RMSE for the estimation of the path separation $c\Delta\tau$. (**a**) is with $\Delta\phi = \pi/3$ and (**b**) is with $\Delta\phi = 2\pi/3$.

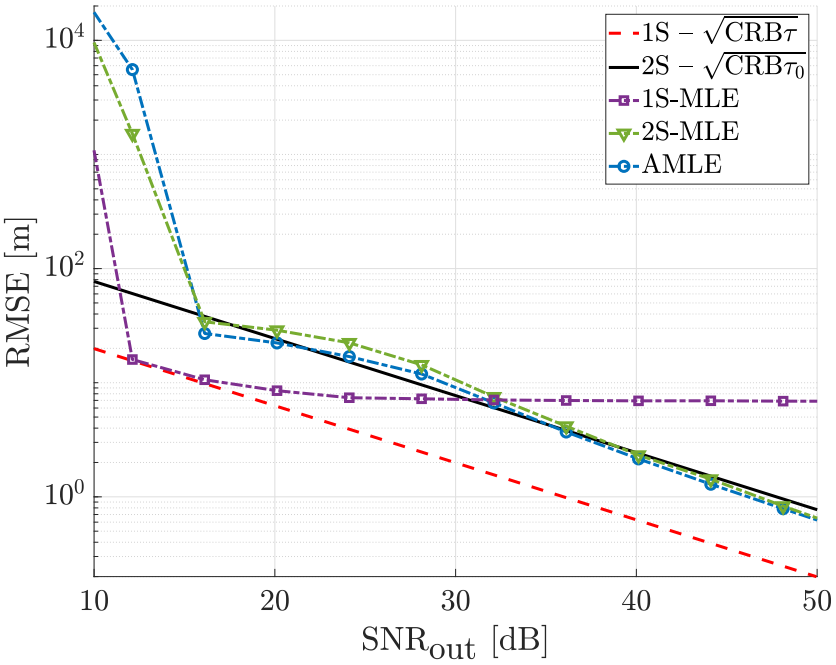

(**a**)

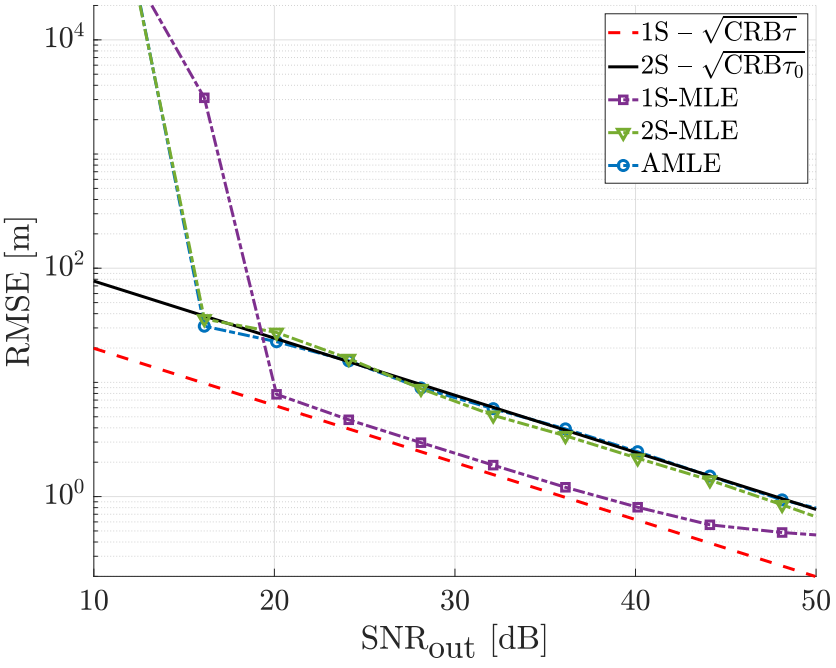

(**b**)

Figure B.6: RMSE for the estimation of the main signal time delay $c\tau_0$ with AMLE, 2S-MLE and 1S-MLE. (**a**) is with $\Delta\phi = \pi/3$ and (**b**) is with $\Delta\phi = 2\pi/3$.